Journal of Alloys and Compounds 545 (2012) 144–147

Contents lists available at SciVerse ScienceDirect

Journal of Alloys and Compounds

journal homepage: www.elsevier.com/locate/jalcom

The atomic and electronic structure of amorphous BP_4

Wei Liu [a], Fengchun Pang [b,c], Hailing Tu [a,*], Xianbin Li [c,*], Xiaoping Su [a], Shuyu Zhang [a], Chengsong Huo [a], Hai Yang [a]

[a] General Research Institute for Nonferrous Metals, Beijing 100088, PR China
[b] College of Physics, Jilin University, Changchun 130023, PR China
[c] State Key Laboratory on Integrated Optoelectronics, College of Electronic Science and Engineering, Jilin University, Changchun 130012, PR China

ARTICLE INFO

Article history:
Received 11 July 2012
Accepted 5 August 2012
Available online 16 August 2012

Keywords:
Boron phosphide
First-principles simulation
Electronic structure
PACVD

ABSTRACT

First-principles simulation and PACVD experiment are used to reveal the atomic and electronic structure of BP_4. With melting–quenching technique in molecule dynamics, for the first time we obtain the microscopic atomic picture for the amorphous BP_4. Here, boron essentially retains a coordination number of 4 and sp^3 electronic bonding whereas phosphorus has a lower coordination number of 3.2 and coexistence of sp^3 and p electronic bonding. The cohesive energy of the present amorphous BP_4 model is up to −5.32 eV/atom which is 1.6 times stronger than −3.37 eV/atom of the usual protected *c*-ZnS.

1. Introduction

Boron phosphide (BP) is a III–V semiconductors with zincblende (ZB) structure [1]. BP exhibits high synthesis temperature of 1130 °C and high melting point of 3000 °C [2,3]. It has attracted great interests on the mechanical properties due to its high hardness. More recently, many efforts have been made to fabricate BP thin film, since it can be used as a protective coating for high velocity infrared transmitting substrates, for example ZnS and Ge [4,5]. Different techniques, such as reactive sputtering (RS), metal organic chemical vapor deposition (MOCVD) and plasma assisted chemical vapor deposition (PACVD), have been reported to prepare BP thin film [6,7]. Among these methods, PACVD is the most popular because it can deposit BP thin film on the surface of optical device with large area and special geometry at low temperature (<500 °C) [5,8]. The BP thin film produced by PACVD is amorphous and non-stoichiometric, BP_x, where x was about 4–8. It is widely accepted that the microstructure of the amorphous BP_x is sustained by the random network of P polymer, which is pinned by B atoms [4,9]. While the microscopic atomic structure of the amorphous BP_x thin film is still too difficult to be observed from experiment.

The theoretical work on ZB BP have been extensively performed, mostly carried out by Wentzcovitch et al. [10,11], Alves et al. [12] and Ferhat et al. [13,14]. Specifically, the structural and electronic properties of ZB BP have recently, calculated by Ferhat [15–17], Zaoui [15–17] and other research group [18] by using first-principles methods based on the density functional theory (DFT). However, there is no investigation on the microstructure of the amorphous BP_x thin film by theoretical calculation. First-principles MD simulation can provide unique insights on the structural evolution and especially obtaining amorphous structure [19]. Herein, we use first-principles MD simulation combined with PACVD experiment to reveal the microscopic atomic structure of amorphous BP_x thin film.

2. Methods and computational details

We use the first-principles MD and structural optimization to reveal the atomic image and electronic structure of amorphous BP_4 thin film. In the MD simulation, the melting–quenching (M–Q) method, which will be detailed later, is used to obtain the model of amorphous BP_4. The density functional theory with the generalized gradient approximation [20] is employed, as implemented in the VASP code [21,22]. The electron–ion interaction is described by the frozen-core all-electron projector augmented wave (PAW) method [23]. An energy cutoff of 350 eV is used for the plane wave expansion. Γ point is used in the Brillouin zone sampling. In the MD simulation, we used the canonical *NVT* ensemble, in which the Nosé–Hoover thermostat is used to control the temperature [24,25].

3. Results and discussion

We prepare BP_x thin film on the substrate of ZnS at 450 °C by PACVD and confirm the x value by auger electron spectroscopy (AES). Fig. 1a and b are the surface and longitudinal analysis of BP_x thin film by AES. It can be seen that, apart from B and P atoms, O and C atoms also detected on the surface. With the increasing of sputtering time, the concentration of O and C atoms decreases, while the concentration of B and P atoms increases. When the

* Corresponding authors.
E-mail addresses: tuhl@grinm.com (H. Tu), lixianbin@jlu.edu.cn (X. Li).

0925-8388/$ - see front matter © 2012 Elsevier B.V. All rights reserved.
http://dx.doi.org/10.1016/j.jallcom.2012.08.022

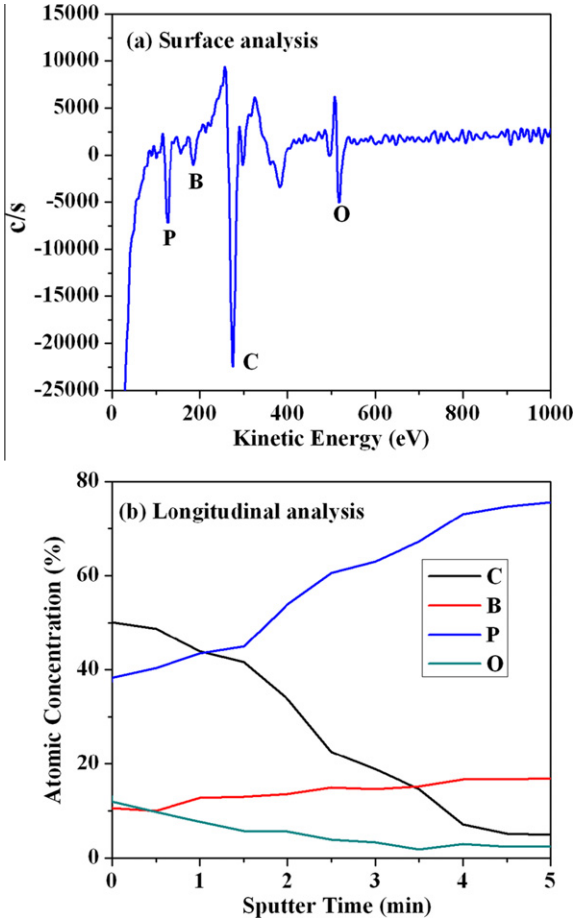

Fig. 1. Surface and longitudinal analysis of BP film by Auger electron spectroscopy (AES). (a) Surface analysis and (b) longitudinal analysis.

sputtering time is over 4 min, the number of O and C atoms is much lower than that of B and P atoms and the ratio of P and B atoms reaches equilibrium, about 4. We also obtained this results by XPS analysis [26]. To predigest the simulation, we ignore the existence of O and C atoms. Therefore, the x value of BP_x is 4 (BP_4).

First, for the convenience of model establishment, the ZB structure is used and a supercell of BP_4 with 216 atoms (43 B, 173 P) is constructed as presented in Fig. 2a. Second, to estimate the density close to the one of BP_4, structural optimization of the starting ZB BP_4 is carried out. Finally, we obtain the density of the relaxed BP_4 is 0.0641 atom/Å^3, which is 25.1% lower than that of ideal ZB BP (0.0856 atom/Å^3). In fact, the covalent radius of P (1 Å) is bigger than that of B (0.85 Å), so when the concentration of P increases the density of BP_4 would obviously decreases. Before the MD simulation, we find an interesting phenomenon. Only adjusted by structural relaxation, the starting model of BP_4 appears a certain degree of amorphization (Fig. 2b). That is to say losing long-range order for the component of BP_4 is quite easy. We define this relaxed BP_4 as natural amorphous BP_4, abbreviated as n-BP_4. As can be seen from Fig. 2b, compared with ZB BP_4 (Fig. 2a), the local optimized BP_4 (n-BP_4) exhibits the disordered structure. The exact degree of order for ZB BP_4 and n-BP_4 is demarcated by the pair correlation functions (PCF) in Fig. 3a. We can see that, when the atomic distance is over 7 Å, there is no any visible feature of order degree for n-BP_4, which indicates that n-BP_4 is indeed disordered. This character is consistent with our PACVD experiment that BP_4 sample is indeed amorphous.

The above simulation just indicates the tendency of losing long-range order for BP_4 but still record the short-range character from the starting ZB structure, hence we use M–Q method in MD to further research the more actual model of amorphous BP_4. The process of M–Q is as followed. First, BP_4 is melt at 4000 K with 2000 steps (3 fs/step) MD simulation, which makes BP_4 fully diffuse to eliminate the memory effect of original ZB structure. Second, BP_4 is quenched to 300 K with 6000 steps (1 fs/step). Third, the geometry optimization is implemented to the quenched structure in order to amend the volume of BP_4 during *NVT* MD. Fig. 2c shows the microscopic atomic picture of amorphous BP_4 by M–Q method. From Fig. 2c, it can be seen that the present model of amorphous BP_4 both loses the feature of long-range order and the character of original ZB structure. Fig. 3a also shows the PCF for BP_4 with M–Q method (termed mq-BP_4 thereof). It exhibits that, when the atomic distance is greater than 5 Å, there is also no any visible feature of order degree for mq-BP_4. After high-energy melting, the atoms of mq-BP_4 are fully diffusive. Therefore, the local structure of amorphous mq-BP_4 is quite different from that of n-BP_4. The most striking difference between mq-BP_4 and n-BP_4 is that the new peaks appear at 1.74 Å and the peak at 3.30 Å shifts to left, which means that the local neighbors of mq-BP_4 become a slight closer. Between the short and middle atomic distance, 2–7 Å, the n-BP_4 maintains a large degree of crystal structure but mq-BP_4 does not. As mq-BP_4 does not have the memory effect of original ZB structure, it is a typical representation for amorphous BP_4. We take mq-BP_4 for further analysis.

In order to detailed demarcate the PCF for different atomic pairs and their weight, we separate the total PCF of mq-BP_4 to partial PCF (g_{ab}) and then multiply g_{ab} by their corresponding atomic density, as shown in Fig. 3b. Three peaks in the nearest neighbors, B–B bonds at 1.74 Å, B–P bonds at 1.97 Å and P–P bonds at 2.25 Å, are easily distinguished, which correspond to the sum of the covalent radius of 1.70 Å (B–B), 1.85 Å (B–P) and 2.00 Å (P–P). Based on the partial PCFs, we get the coordination number (CN) for B and P element, respectively. For B atom total CN(B) of 3.96 includes 0.72 of B–B and 3.24 of B–P whereas for P atom total CN(P) of 3.24 includes 0.81 of P–B and 2.43 of P–P. Fig. 3c is the distribution function of bond angle for B and P atom in mq-BP_4. The bond angles of B atom maintain the sp^3 hybrid bonding characteristics of the ideal ZB BP with 109.47°. However, the bond angles of P atom significantly deviate from the original sp^3 feature and also a shoulder around 90° can be observed. This phenomenon is consistent with the situation of coordination. For B atom, the most coordinated atoms are still P atoms as the case in ZB BP, so sp^3 hybrid bonding is still a main effect. For P atom, the coordination number of P is obviously larger than that of B, so the hybrid effect becomes weaker. Fig. 3d further shows the element- and orbital-dependent density of state (DOS) for mq-BP_4. We can see that the obvious separation of s- and p-orbital electronic states for P element is in contrast to the case for B element. The bond angle of around 90° from P element indeed reflect the enhancement of p-orbital states near valence band maximum. Fig. 2d further highlights the 90° square ring in amorphous mq-BP_4. These deformed or distorted square rings are mainly composed of P atoms. This is a direct proof of existence of p-orbital bonding for P atoms. Therefore, P atoms should both have original sp^3 and new p-orbital bonding characters in amorphous BP_4.

4. Conclusions

First-principles MD calculations and PACVD experiments reveal the atomic picture and electronic structure of amorphous BP_4, which have not been addressed before. Upon completion of the work, we learn that losing long-range order for BP_4 is quite easy, as reflected by n-BP_4. Through M–Q technique in MD, mq-BP_4

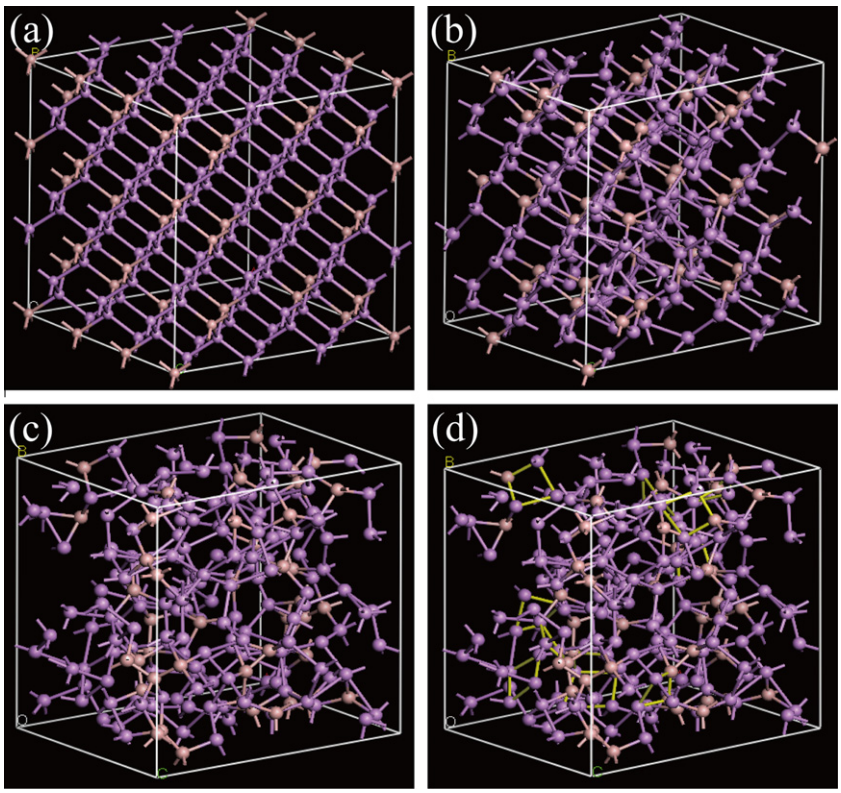

Fig. 2. (a) Original atom model of BP_4 based on zincblende structure; (b) atomic model of BP_4 after optimization from (a); (c) atomic model of BP_4 by melting–quenching (M–Q) method and (d) square ring close to 90° (yellow color) in atomic model of BP_4 by M–Q method. P and B atoms are marked by purple and brown ball, respectively. (For interpretation of the references to colour in this figure legend, the reader is referred to the web version of this article.)

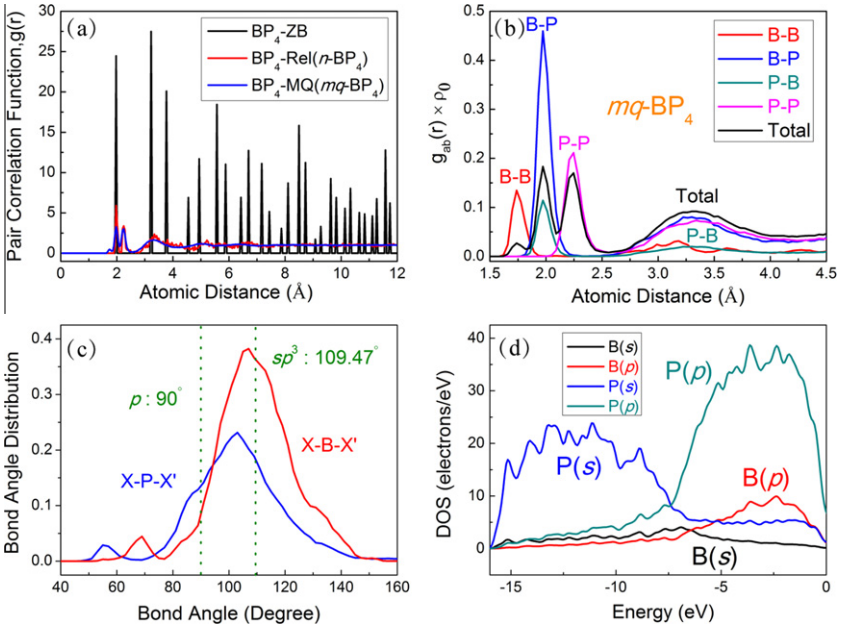

Fig. 3. (a) Pair correlation functions of zincblende BP_4 (BP_4-ZB), natural amorphous BP_4 (n-BP_4) and BP_4 by melting–quenching method (mq-BP_4); (b) partial pair correlation functions of mq-BP_4 for different atom pairs multiplied by the corresponding atomic density; (c) atomic bond angle distribution function of mq-BP_4, the blue line is for P atoms and the red line is for B atoms; (d) the element- and orbital-dependent density of state (DOS) for mq-BP_4. (For interpretation of the references to colour in this figure legend, the reader is referred to the web version of this article.)

model, a typical representation for amorphous BP_4, is obtained. In mq-BP_4, B atoms retain sp^3 electronic bonding while P atoms have coexistence of sp^3 and p bonding. The cohesive energy reflecting bond strength of material is −5.32 eV/atom for mq-BP_4 and −3.37 eV/atom for c-ZnS. This is consistent with the fact that amorphous BP_4 can be employed to protect c-ZnS.

Acknowledgments

This work was supported by NSFC (Contract No. 11104109). We also thank the High Performance Computing Center (HPCC) of Jilin University for calculation resource.

References

[1] D.W. Wheeler, R.J.K. Wood, Surf. Coat. Technol. 200 (2006) 4456.
[2] N. Amrane, Superlatt. Microstruct. 33 (2003) 9.
[3] S. Dalui, A.K. Pal, Appl. Surf. Sci. 254 (2008) 3540.
[4] K.L. Lewis, J.A. Savage, SPIE 1275 (1990) 46.
[5] D.R. Gibson, E.M. Waddell, K.L. Lewis, SPIE 2286 (1994) 335.
[6] J.M. Mackonski, B. Cimma, J. Lacuve, P. Lapart, SPIE 2286 (1994) 552.
[7] A. Ogwu, T. Hellwig, S. Doherty, D. Haddow, K.P. Möllmann, F. Placido, SPIE 5786 (2005) 130.
[8] D.C. Harris, SPIE Press, Bellingham, WA, USA, 1999.
[9] K.L. Lewis, C.J. Kelly, B.C. Monachan, SPIE 1112 (1989) 407.
[10] R.M. Wentzcovitch, M.L. Cohen, P.K. Lam, Phys. Rev. B 36 (1987) 6058.
[11] R.M. Wentzcovitch, K.J. Chang, M.L. Cohen, Phys. Rev. B 34 (1986) 1071.
[12] H.W.L. Alves, K. Kunc, J. Phys.: Condens. Matter 4 (1992) 6603.
[13] M. Ferhat, A. Zaoui, M. Certier, H. Aourag, Physica B 252 (1998) 229.
[14] B. Bouhafs, H. Aourag, M. Ferhat, M. Certier, J. Phys.: Condens. Matter 11 (1999) 5781.
[15] D. Touat, M. Ferhat, A. Zaoui, J. Phys.: Condens. Matter 18 (2006) 3647.
[16] A. Zaoui, F.E.H. Hassan, J. Phys.: Condens. Matter 13 (2001) 253.
[17] M. Briki, M. Abdelouhab, A. Zaoui, M. Ferhat, Superlatt. Microstruct. 45 (2009) 80.
[18] O. Arbouche, B. Belgoumène, B. Soudini, Y. Azzaz, H. Bendaoud, K. Amara, Comput. Mater. Sci. 47 (2010) 685.
[19] X.B. Li, X.Q. Liu, X. Liu, D. Han, Z. Zhang, X.D. Han, H.B. Sun, S.B. Zhang, Phys. Rev. Lett. 107 (2011) 0155011.
[20] J.P. Perdew, K. Burke, M. Ernzerhof, Phys. Rev. Lett. 77 (1996) 3865.
[21] G. Kresse, J. Furthmüller, Phys. Rev. B 54 (1996) 11169.
[22] G. Kresse, J. Furthmuller, Comput. Mater. Sci. 6 (1996) 15.
[23] G. Kresse, D. Joubert, Phys. Rev. B 59 (1999) 1758.
[24] D.M. Bylander, L. Kleinman, Phys. Rev. B 46 (1992) 13756.
[25] S. Nosé, Prog. Theor. Phys. Suppl. 103 (1991) 1.
[26] W. Liu, H.L. Tu, H. Yang, S.Y. Zhang, L.Q. Yan, C.S. Huo, X.P. Su, J. Alloys Comp. 538 (2012) 169.